International Journal of General Medicine

Dovepress

open access to scientific and medical research

Open Access Full Text Article

ORIGINAL RESEARCH

Modified TI-RADS Coupled with BRAFV600E Enhances Diagnostic Efficiency in Papillary Thyroid Carcinoma: Prospective Study

Jing Wang, Hong Cheng, Xu Li

Department of Ultrasound, Bishan Hospital of Chongqing, Bishan Hospital of Chongqing Medical University, Chongqing, 402760, People's Republic of China

Correspondence: Xu Li, Tel +86-13637920860, Email lxzk11110000@163.com

Background: Thyroid disorders, relatively common diseases of the endocrine system, have risen gradually in recent years. Early detection and accurate diagnosis of thyroid cancer hold exceptional importance. This study aimed to determine the efficacy of a modified TI-RADS and BRAFV600E mutation testing for thyroid cancer (PTC) diagnosis.

Methods: Ninety five thyroid nodules (48 benign and 47 malignant) from 81 patients were examined using Kwak Thyroid Imaging Reporting and Data System (TI-RADS) were subjected to shear wave elasticity (SWE), BRAFV600E genotyping and fine needle aspiration (FNA) cytology.

Results: The modified TI-RADS exhibited superior diagnostic accuracy compared to TI-RADS in differentiating benign nodules from malignant thyroid nodules. Moreover, the AUC of modified TI-RADS in conjunction with BRAFV600E was the highest at 95% CI (0.898–0.992, p=0.003), surpassing other diagnostic methods in enhanced sensitivity and maintaining high specificity.

Conclusion: The diagnostic efficiency of this combination surpassed that of individual diagnostic methods.

Keywords: modified TI-RADS, shear wave elasticity, stiff rim sign, BRAFV600E, papillary thyroid cancer

Background

The thyroid gland, composed of two interconnected lobes, is the largest endocrine organ, weighing 20–30 g in adults. Occurring in approximately 4%-7% of cases, thyroid lesions are a prevalent feature.[1] Thyroid papillary microcarcinoma (PTMC), characterized by a tumor diameter of less than or equal to 10 mm, has shown an escalating trend in incidence based on the Surveillance Epidemiology and End Results (SEER) database from 1990 to 2019. Specifically, in China, thyroid cancer diagnoses soared from 10,030 cases to 39,079 during this period with the steepest increase emanating from PTMC. However, mortality remained stable at 1.4%, showing no significant increment.[2] The 2015 American Thyroid Association Management Guidelines for Adult Patients with Thyroid Nodules and Differentiated Thyroid Cancer recommend active follow-up surveillance may be considered as an alternative to surgery for low-risk differentiated thyroid cancer, such as less aggressive papillary thyroid microcarcinoma (PTMC).[3] Therefore, early diagnosis and precise identification of thyroid cancer is particularly important. Fine needle aspiration (FNA) can enhance the diagnostic compliance rate, but is operator-dependent and has an uncertain rate of over 15% for cytologic results.[4] A method to identify aggressive features is needed.

Shear wave elastography (SWE) is a novel imaging technique reflecting tissue stiffness, overcomes the disadvantages of operator-dependent pressure elastography, offering real-time, quantitative, less operator-dependent, and highly reproducible results. It is widely used in clinical settings, particularly for superficial organ studies. In numerous studies,[5–9] SWE has demonstrated high specificity and accuracy in thyroid disease diagnosis, enhancing early detection of malignancy. The 2015 American Thyroid Association Management Guidelines advocate molecular testing for nodules with indeterminate cytologic findings.[10] Studies indicate BRAFV600E is beneficial in assessing thyroid nodules benignity,[11,12] the presence of extra-thyroid tissue invasion, and central neck lymph node metastasis. However, each

Received: 27 December 2023
Accepted: 9 June 2024
Published: 10 July 2024

test technique has its own limitations. This study aims to investigate the predictive ability of SWE combined with BRAFV600E for papillary thyroid cancer, integrating multiple test parameters to more accurately reflect thyroid nodule biology and aid clinical management.

Methods

Subjects

This prospective study was reviewed and approved by the Ethics Committee following the guidelines of Helsinki Declaration of 1964. Written informed consent was obtained from each participant. From April 2020 to October 2020, ultrasound reports for 155 thyroid nodules from 137 patients were used to classify thyroid nodules as Category 4 according to TI-RADS. The inclusion criteria were: available data from conventional 2D ultrasound and real-time SWE, TI-RADS thyroid nodule classification, clear cytology or pathological findings, and BRAFV600E gene test results. Exclusion criteria were as follows: any history of radiotherapy, chemotherapy or interventional therapy, nodules with large calcified foci, and nodules with a lower edge depth >4 cm adjacent to large pulsating blood vessels in the neck. Excluding nodules due to poor image quality and incomplete data, 95 thyroid nodules from 81 patients were finally included in the analysis. The flow chart for patient selection is shown in Figure 1.

Instruments

Conventional ultrasound and SWE were performed using a color Doppler ultrasound instrument from the Aixplorer US system (SuperSonic Imagine, Aix-en-Provence, France) and an SL15-4 multi-frequency linear probe. Standard thyroid device settings were used. ARMS-PCR kit testing BRAF V600E, a fully automated medical PCR analyser for gene amplification.

Greyscale Ultrasound and SWE Examination

Patients were placed in a decubitus position, the anterior cervical region was fully exposed, transverse and longitudinal sections of both lobes and isthmus of the thyroid were comprehensively examined, and the size, location, 2D greyscale features (composition, morphology, margins, presence of microcalcifications and continuity of the outer envelope the thyroid, etc.) and Doppler ultrasound features of the largest section of each nodule were recorded in detail, and the nodules were selected for malignancy according to the 2017 edition of Kwak TI-RADS classification criteria for greyscale ultrasound malignant features (solid, hypoechoic, aspect ratio>1, outer envelope discontinuity, microcalcifications, etc.), the nodules were evaluated for malignant risk, and nodules with 4 categories were selected for SWE, with adequate application of coupling agent, no pressure on the probe, and the patient was instructed to relax, not to extend the neck so as not to exert additional pressure on the thyroid gland, breathe calmly, not to make swallowing movements, and take the largest section of the nodule. Start the SWE measurement kit with the default elasticity scale of 0–100 kPa, cover the entire nodule and surrounding normal glandular tissue, and observe elasticity characteristics, whether the image is homogeneous, and whether there is a "stiff rim sign" around the nodule (Figure 2). Emax and Emean were recorded.The "stiff rim sign" was defined as a ring-shaped or semi-ring-shaped band around the nodule that was significantly harder than the adjacent normal thyroid gland on the elastogram. The elasticity sampling frame was adjusted to measure the elasticity parameter at the hardest part of the nodule with 2 mm as the region of interest (ROI) diameter, the elasticity value of the normal gland surrounding the nodule was measured, and the ratio of the two was calculated. All values were measured three times by two physicians with more than 5 years of extensive experience in thyroid nodule diagnosis, and the mean value was finally calculated and recorded.

Image Analysis

Modified the Kwak TI-RADS classification with the SWE technique's elasticity map characteristics: If the resilience map has a "stiff rim sign", the TI-RADS category is upgraded (category 4a to 4b, 4b to 4c, or 4c to 5). If there were no "stiff rim signs" on the elasticity map, the TI-RADS category was downgraded (5 to 4c, 4c to 4b, 4b to 4a, or 4a to 3). Changes in the risk of malignancy of readjusted TI-RADS masses, particularly when TI-RADS was downgraded from Category 4 to Category 3 or upgraded from Category 4 to Category 5, changed the treatment decision for thyroid masses.

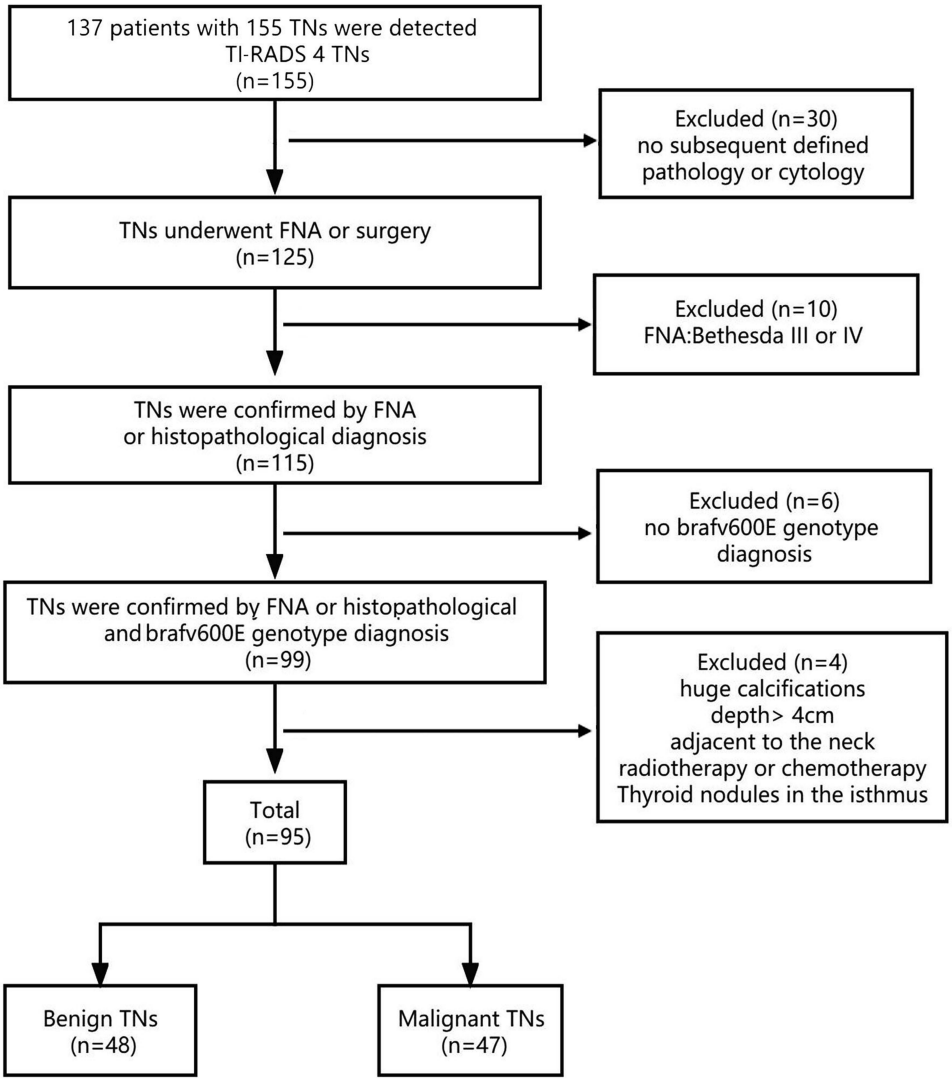

Figure 1 Diagram of the selection of patients with thyroid nodules.

BRAFV600E Mutation Analysis

After the location of the suspected nodule is determined under ultrasound guidance, routine disinfection, towel laying, and anaesthesia are performed, and the tissue is repeatedly needled by an experienced thyroid surgeon using a fine needle. Some tissues were coated for cytology, some tissues were extracted from DNA according to kit instructions, and gene mutations were determined by real-time quantitative fluorescence PCR.

Statistical Analysis

SPSS25 was employed for data analysis. Data normality was initially assessed via Kolmogorov–Smirnov (K-S) test, mean±SD was used to represent normally distributed measurement data, and the independent *t*-test scrutinized sample data differentiating malignant from benign thyroid nodules. Emax, Ratio, and "stiff rim sign" were illustrated on the operational characteristic curve (ROC) of diagnosing malignant thyroid nodules using elasticity-related parameters, along with the diagnostic threshold, sensitivity, and specificity. ROC curves were utilized to compute the area under the curve (AUC) of TI-RADS, Modified TI-RADS, BRAFV600E, and Modified TI-RADS+BRAFV600E, and to evaluate their diagnostic efficacy in distinguishing malignant and benign thyroid nodules. Statistical significance was set at $p < 0.05$.

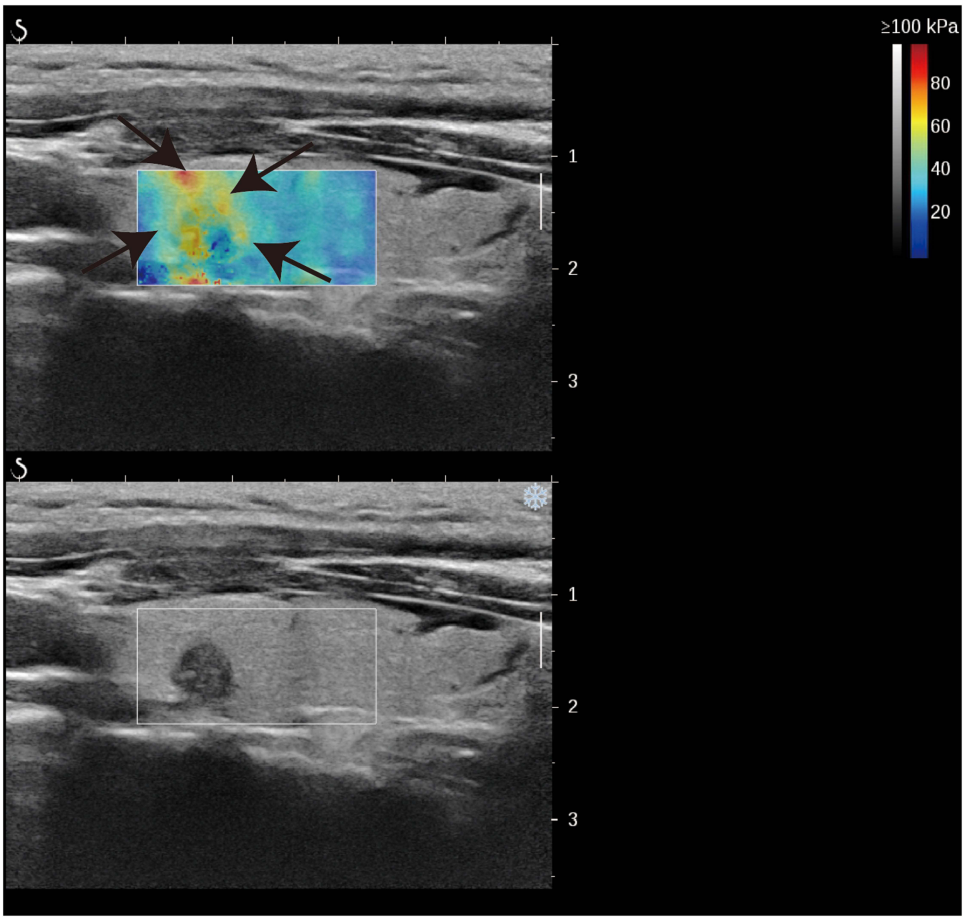

Figure 2 The stiff rim (arrow) is a ring light banded area where the edge of the nodule is harder than the surrounding normal thyroid glands.

Results

Pathological results

Among the 95 thyroid nodules, 48 were benign; 47 were malignant papillary carcinoma, with 16 cases of cervical lymph node metastasis and 31 cases without cervical lymph node metastasis (Figures 3 and 4). A total of 16 patients had nodules that measured ≥1 cm (1.38± 0.34 cm), 25 had nodules that measured < 0.5 cm (0.26± 0.17 cm), and 54 had nodules that measured between 0.5 and 1 cm (0.71 ± 0.38 cm).

Comparison of Quantitative Parameters of Ultrasound Elastography Between Thyroid Nodules of Different Pathological Types and BRAF Genotypes

Results of statistical analyses showed that the estimated Emax, Emean and Ratio values were higher in the benign group than in the malignant group (Table 1) and in BRAF V600E mutation group than in the wild type group (Table 2), with a significant difference observed ($p < 0.05$).

The Relationship Between TI-RADS, Modified TI-RADS, BRAF V600E and Pathological Types

In SWE, modified TI-RADS reduced categorization for 46 thyroid nodules lacking the stiff rim sign and increased it for 49 nodules exhibiting this sign. This resulted in an improved diagnostic sensitivity by converting 81% of malignant nodules into Category 5. Furthermore, the revised system accurately identified 23 Category 4-upgraded malignant nodules, translating to 91% of all malignancies. It outperformed TI-RADS significantly in differentiating benign thyroid

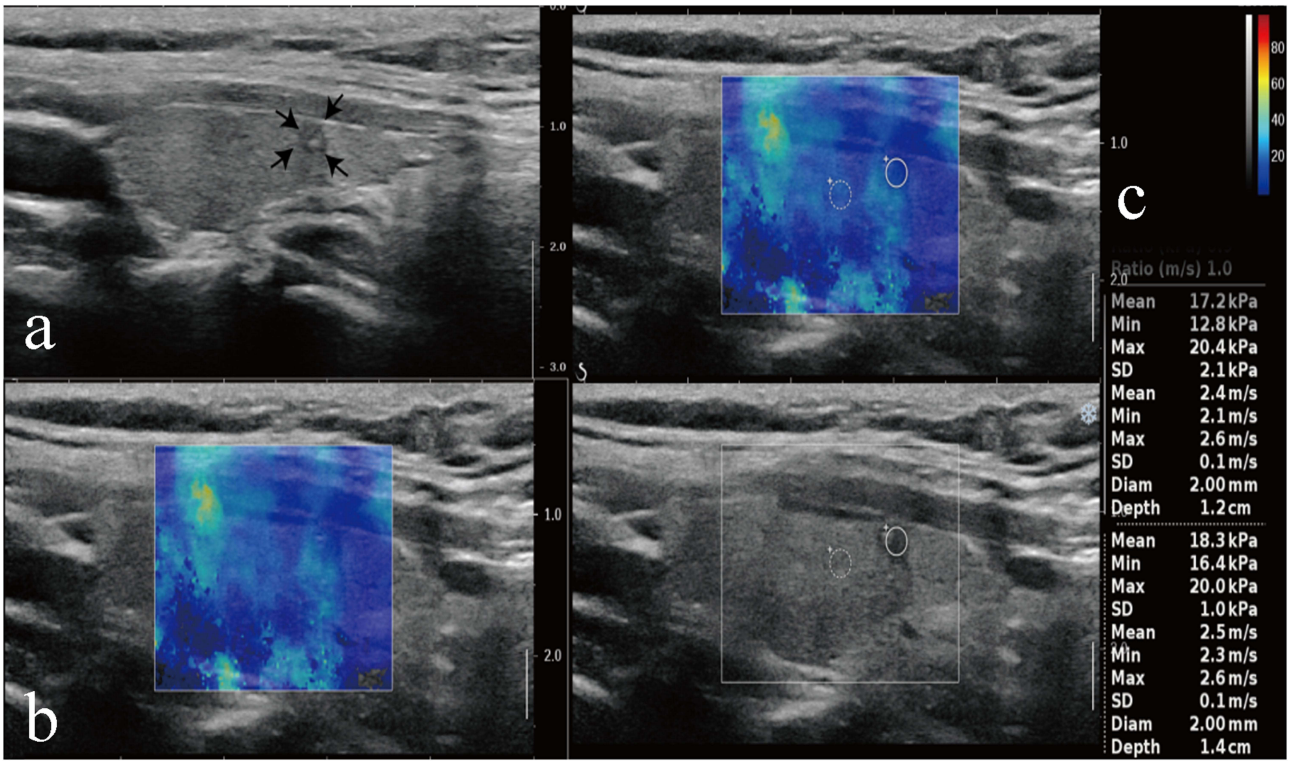

Figure 3 A representative image of a 49-year-old woman with benign FNA results and wild-type BRAF V600E. (**a**) CUS image showed hypoechogenicity, microcalcification, and solid component features in the longitudinal plane. (**b**) The nodule did not have a stiff rim. (**c**) SWE max and SWE ratio are shown on the elastic image as 20.4 KPa and 1.0kPa, respectively. Arrows denote nodule size and location. Color Doppler imaging distinguishes red blood flowing towards the transducer from blue blood receding.

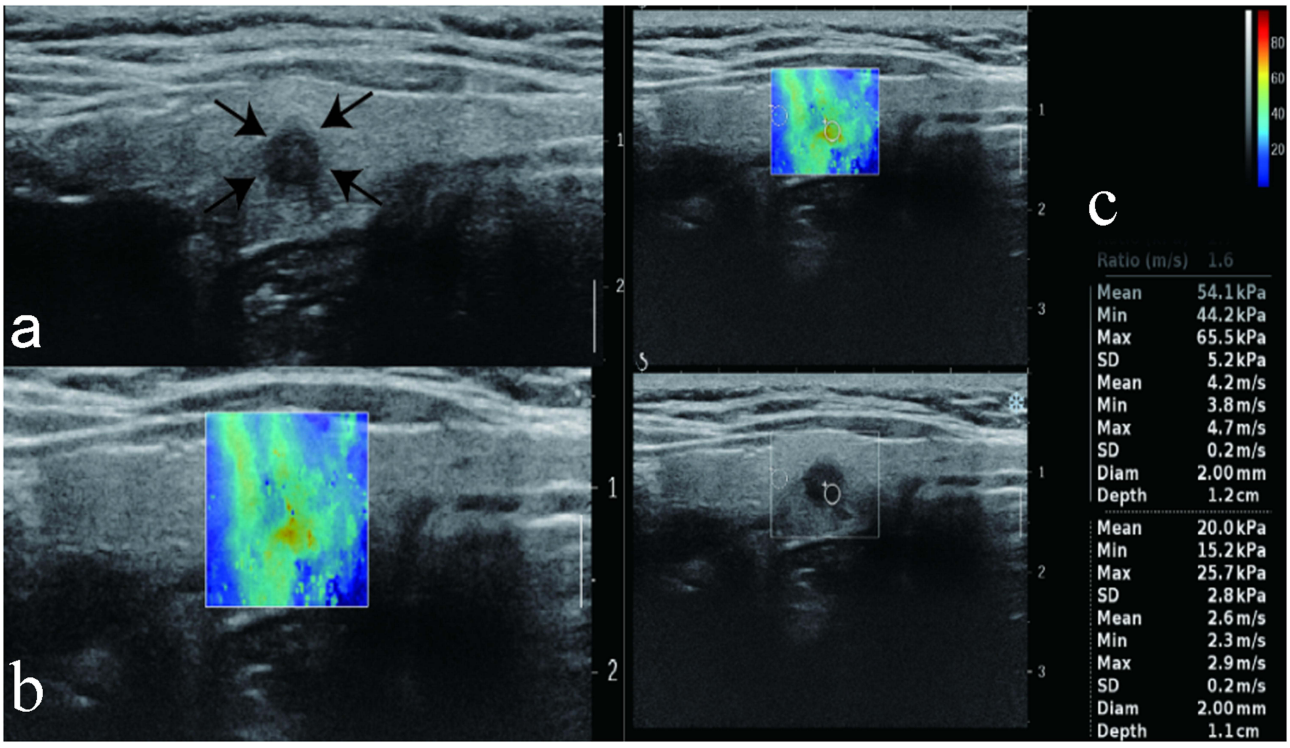

Figure 4 A representative image of a 52-year-old woman with mutation type BRAF V600E and the pathological result PTC. (**a**) The CUS image showed hypoechogenicity, an irregular boundary, and microcalcification features in the longitudinal plane. (**b**) The nodule had a stiff rim. (**c**) SWE max and SWE ratio are shown on the elastic image with values of 65.5 kPa and 1.6 kPa, respectively. Arrows denote nodule size and location. Color Doppler imaging distinguishes red blood flowing towards the transducer from blue blood receding.

Table 1 Comparison of the Elastic Parameters Among Thyroid Nodules of Different Pathological Types

Groups	Emax (Kpa)	Emean (pka)	Ratio
Benign	33.98±18.63	22.32±18.30	1.12±0.36
Malignant	52.92±34.43	40.20±32.40	1.46±0.56
p	0.017	0.003	0.016

Table 2 Comparison of the Elastic Parameters Among Thyroid Nodules of Different BRAF Genotypes

Groups	Emax (Kpa)	Emean (pka)	Ratio
Wild	34.93±19.80	24.30±23.38	1.17±0.48
Malignant	54.44±35.25	38.75±35.89	1.44±0.48
p	0.032	0.001	0.017

nodules from malignant ones. A total of 54 BRAF V600E thyroid nodules were examined: 44 benign, 10 malignant, and 4 with central neck lymph node metastases. Of these, mutant BRAF V600E thyroid nodules had a significantly higher risk of malignancy and lymph node metastases compared to wild-type nodules (Table 3).

Diagnostic Efficacy of SWE in the Diagnosis of PTC

Comparing Emax, Ratio, and the "stiff rim sign" with pathology report results, after a comprehensive analysis of the ROC curve (Figure 5), the AUC of malignant nodules was statistically significant ($p < 0.001$). The best diagnostic cut-off for Emax and Ratio was 34.18 kPa and 1.15, respectively, with sensitivities of 72.3% vs 66.0%, specificity of 66.7% vs 70.8%. The AUC for diagnosis of the "stiff rim sign" was 0.790, with a sensitivity of 80.9% and a specificity of 77.1%, and best diagnostic efficacy for PTC.

Comparison of the Diagnostic Efficacy of TI-RADS, Modified TI-RADS, BRAFV600E and the Combined Application of Modified TI-RADS and BRAFV600E for PTC

The ROC curves showed that modified TI-RADS outperformed TI-RADS in diagnosing malignant thyroid nodules (Figure 6); the AUC of modified TI-RADS and BRAFV600E was similar at 95% CI (0.808–0.893) and 95% CI (0.809–0.895), but BRAFV600E specificity was highest at 95% CI (87.02–96.29). The AUC of modified TI-RADS combined with BRAFV600E was highest at 95% CI (0.898–0.992), p=0.013 which was superior to any diagnostic method in terms of improved sensitivity while ensuring high specificity (Table 4).

Table 3 The Relationship Between TI-RADS, Modified TI-RADS, BRAF V600E and Pathological Types

TI-RADS		Modified TI-RADS		BRAF V600E		Pathological results		Central lymph node	
Category	n	Category	n	Wild	Mutation	Benign	Malignant	Benign	Malignant
TR 4a	4	3	1	1	0	1	0	1	0
		4b	3	1	2	0	3	1	2
TR 4b	52	4a	29	23	6	25	4	28	1
		4c	23	10	13	8	15	18	5
TR 4c	39	4b	16	13	3	12	4	15	1
		5	23	6	17	2	21	16	7

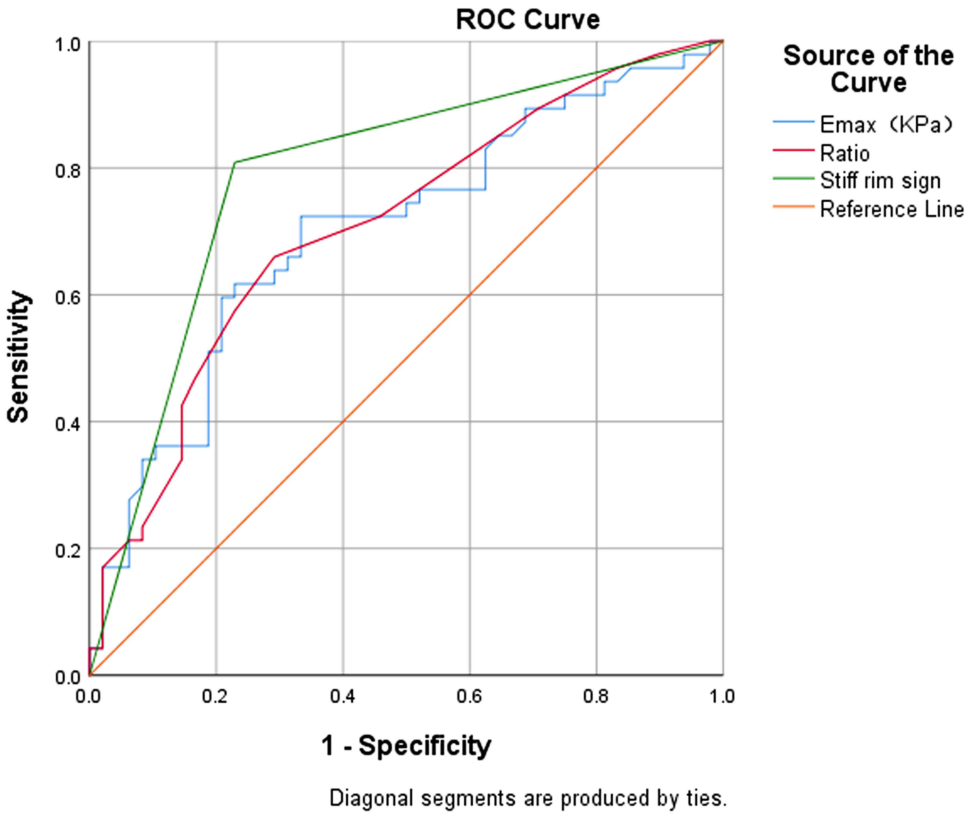

Figure 5 The receiver operating characteristic curves of shear-wave elastic parameters for the prediction of PTC.

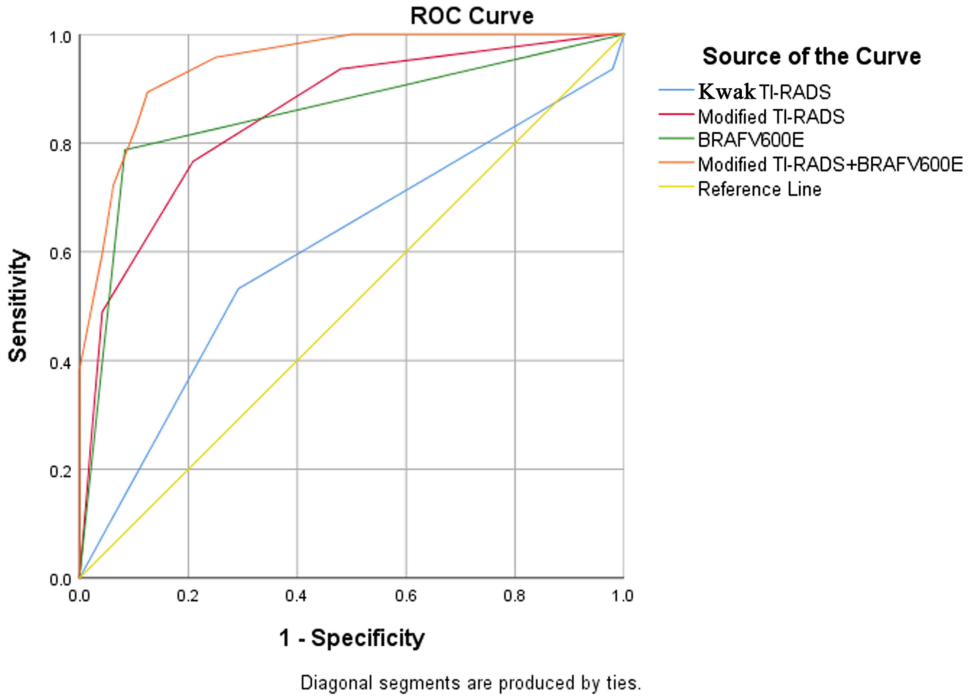

Figure 6 The receiver operating characteristic curves of different test techniques for the prediction of PTC.

Table 4 Comparison of the Diagnostic Efficacy of TI-RADS, Modified TI-RADS, BRAFV600E and the Combined Application of Modified TI-RADS and BRAFV600E for PTC

Groups	AUC	Sensitivity (%)	Specificity (%)
TI-RADS	0.602 (0.572–0.632)	53.2 (50.54–55.86)	70.8 (67.26–74.34)
Modified TI-RADS	0.850 (0.808–0.893)	76.6 (72.77–80.43)	79.2 (75.24–83.16)
BRAFV600E	0.852 (0.809–0.895)	78.7 (74.77–82.64)	91.7 (87.02–96.29)
Modified TI-RADS+BRAFV600E	0.945 (0.898–0.992)	89.4 (84.93–93.87)	87.5 (83.13–91.88)
p	0.013	0.002	0.045

Discussion

Thyroid carcinoma (TC), accounting for one percent of all carcinomas, predominantly affects women. Thyroidectomy (TT) and subtotal thyroidectomy (STT) remain the primary surgical procedures.[13] Technological advances in surgery have been rapid and ongoing in recent years. One significant development is the incorporation of IoT concepts into surgical practice, promoting telesurgery and telementoring.[14] Rapid early diagnosis portends favorable outcomes.

Currently, ultrasound-guided fine needle aspiration (US-FNA) remains the most effective and tolerable technique for diagnosing malignancy.[15] The Bethesda System for Reporting Thyroid Cytopathology (BSRTC) utilizes six categories for thyroid cytology reporting: I-nondiagnostic, II-benign, III-atypia of undetermined significance / follicular lesion of undetermined significance, IV-follicular neoplasm / suspicious for follicular neoplasm, V-suspicious for malignancy, and VI-malignant.[16] A study found that 44.77% (522/1166) of patients with a Bethesda II FNA underwent thyroid surgery, with incidental malignancy identified in 1.53% (8/522) of these cases.[16] Given its heterogeneity and inconsistent reporting, Bethesda category III is the most contentious. Nodules falling within Bethesda categories III–IV carry an overall malignancy risk of between 15 and 40%.[17] In this study, 47 malignant nodules were identified, with 17 nodules≤5 mm accounting for 36.17% of the total malignant nodules, including 4 cases of combined cervical lymph node metastasis, indicating that nodules≤0.5 cm are also at risk of metastasis, echoing previous studies.[18] Hence, it is crucial to identify a reliable method for early nodule invasiveness diagnosis, aiding in the pre-FNA screening of suspicious nodules, assessing the necessity of FNA or surgical treatment, avoiding unnecessary examinations, and reducing the underdiagnosis and misdiagnosis of microscopic thyroid cancer.

Kwak's TI-RADS categorization method enhances thyroid nodule management through standardized sonographic description and evaluation, effectively predicting malignancy. However, benign signs can mimic malignancy in certain scenarios. Possible explanations include: Thyroid tissue's loosely arranged nature, causing nodular goiter nodules to frequently develop cystic changes or bleed. Certain nodules tend to collapse over time, transforming into irregular, hypoechoic, solid formations, potentially mimicking microcalcifications. This can lead to confusion with papillary thyroid cancer's acoustic image, potentially misclassifying TI-RADS as Category 4–5. Follicular carcinomas, characterized by follicles of varying differentiation, minimal interstitial components, and subtle fibrosis, often appear isoechoic, non-calcified, non-halo, with clear margins, potentially underrating TI-RADS (as seen in Cao J et al).[19] To counter TI-RADS' limitations, researchers have explored the use of SWE technology, capable of quantifying tissue elasticity in real-time via transverse wave emission, reflecting nodule hardness and assessing cancer risk.[20,21] Malignant nodules typically exhibit complex tissue components rich in mesenchymal elements and prominent fibrosis, containing sand-like particles, while benign nodule cells primarily consist of glia, less fibrous, softer, and highly deformable. According to Hooke's law, softer tissues yield lower Young's modulus values, and stiffer tissues yield higher elastic modulus values. Statistical data from this study indicated that malignant nodule's Emax and Ratio were significantly higher compared to benign thyroid nodules, mirroring their pathological features. However, seven malignant nodules displayed lower Emax and Ratio than the cut-offs for both benign and malignant nodules, including two follicular subtype thyroid cancers with numerous follicles, minimal fibrosis, and increased deformability, thus yielding lower elasticity values. Four nodules were smaller than 0.5 cm, possibly influencing elasticity measurements. One case was associated with hyperthyroidism, potentially linked to abundant blood vessels and proliferating follicular epithelial cells, reducing elasticity values. Two nodules had Emax values exceeding 200 Kp, significantly higher than the group's mean, and were located in the isthmus. This could

be attributed to the isthmus's superficial position, more susceptible to external disturbances, resulting in elevated elasticity values, indicating that isthmus lesions might not be ideal for SWE examination. Most benign nodules with significantly higher Emax than the cut-off were coexisting with Hashimoto's thyroid disease or contained calcification foci. This could be due to significant thyroid tissue fibrosis in Hashimoto's thyroiditis patients, thyroid cell hypoxia and bleeding, and subsequent scarring or calcification, lowering nodule elasticity. Currently, the Emax cut-off values for diagnosing benign and malignant nodules vary widely between 28.2 Kpa-94 Kpa,[22–24] likely influenced by differences in elastic ROI selection among examiners. The complex tissue composition of malignant nodules often leads to calcification and necrosis, resulting in heterogeneous shear wave elastograms, potentially biasing elasticity measurement outcomes.[25] The "stiff rim sign", derived from the principle of fibroblast proliferation by cancer cells, renders the tumour periphery harder due to its exclusion of the nodule's interior condition and resistance towards internal calcification/necrosis influences on elasticity quantification, unrestricted by cutoff values.[26,27] This study found the "Stiff rim sign" to exhibit superior diagnostic prowess amongst three thyroid cancer detection methods using shear wave elasticity. The modified TI-RADS demonstrated significantly enhanced sensitivity and specificity over TI-RADS, thereby enhancing thyroid cancer detection capabilities. These findings align with those of Tan S. et al,[5,24,28] indicating the potential use of the "stiff rim sign" as a malignancy indicator in thyroid nodules. While the shear wave elasticity method holds promise for broader application, nodule size, hormone levels, and location impacts on measured values remain considerations.

Gene mutations impact tumor development and advancement, with BRAF V600E being predominant in PTC,[29] stimulating PI3K/AKT/ mTOR and MAPK/ERK pathways via its interaction with Major Vault Protein, a reliable indicator of the immune microenvironment.[30] BRAF V600E can elevate pro-oncogenic molecule production, enhance cell multiplication, stimulate neoangiogenesis, and reinforce PTC pathogenesis.[31] Statistical evidence indicates that mutant BRAF V600E is related adversely to thyroid nodule malignancy. Analysis revealed two follicular thyroid carcinoma occurrences among ten benign BRAF V600E thyroid nodules.[32] The mutation rate in the classical cell subtype ranges between 90% - 100%, however it's merely 12% - 18% for the follicular subtype.[32] Experimental findings indicate that BRAF V600E-mutated thyroid cancers display higher regional cervical lymph node metastases rates than non-mutated ones, suggesting a strong correlation with thyroid carcinogenesis, extraperitoneal cancer spread, recurrence, and lymph node metastases, echoing prior research.[33,34] This information aids surgeons in determining appropriate surgical strategies during initial procedures.[35,36] Nucera et al's experiments demonstrated that PLX4720, a specific BRAF V600E inhibitor, suppresses BRAF V600E thyroid cancer cell migration and invasion, thereby reducing tumor aggression.[37] Elisei et al observed a higher mortality rate among BRAF V600E-positive PTC patients over a 15-year follow-up period, indicating that BRAF V600E is an independent poor prognostic factor and the sole predictor of persistent disease.[38] Despite these findings, some studies suggest no association between BRAF V600E and lymph node metastases.[29] Chen et al discovered that BRAF V600E-positive PTC patients are more prone to TERTp mutation, which independently predicts unfavorable PTC patient outcomes. Patients harboring both mutations face heightened risk of adverse events when compared to those with a single mutation. Mutation detection could aid in risk classification (BRAF + TERT+ > BRAF − TERT+ > BRAF + TERT−).[39]

This analysis involved thyroid nodules classified as Category 4 under TI-RADS, with limited instances and potential selection bias. Thus, further, comprehensive multicenter regional studies with larger cohorts are required to verify these findings.

Conclusions

In BRAF V600E wild thyroid cancer, except for 2 cases with follicular subtype Emax below the cut-off value, the remaining 8 cases had Emax close to or above the cut-off value, and 87.5% (7/8) of the cases had a "stiff rim sign" in elastography. If BRAF V600E and SWE were applied in combination, all suggested a risk of malignant nodules. The AUC of the combined application of modified TI-RADS and BRAF V600E for the diagnosis of PTC was superior to any diagnostic method in terms of improved sensitivity while ensuring high specificity, and SWE and BRAFV600E could compensate for each other's shortcomings. Therefore, both SWE and BRAFV600E can be used as an important supplement to FNA thyroid cancer diagnostic compliance. Rational clinical selection of screening methods can be highly invasive and avoid clinical puncture and surgery of low-risk nodules at an early stage and reduce the economic and psychological burden of patients.

Abbreviations

PTC, papillary thyroid cancer; TI-RADS, Thyroid Imaging Reporting and Data System; SWE, shear wave elasticity; ROC, operational characteristic curve; AUC, area under the curve.

Data Sharing Statement

All data, models, and code generated or used during the study appear in the submitted article.These are available upon request by contact with the corresponding author.

Ethics Approval and Consent to Participate

This perspective study was reviewed and approved by the Ethics Committee of The Second Affiliated Hospital of Chongqing Medical University and followed the guidelines from the 1964 Declaration of Helsinki.

Approval ID, Scientific Ethics Review No. (69), 2019.

Approval Date,31 December 2019.

An informed consent form was obtained from each participant.

Funding

Project supported by the National Natural Science Foundation of China (Grant No.82071926). The funder had no role in study design, data collection and analysis, decision to publish, and preparation of the manuscript.

Disclosure

The authors of this manuscript declare no relationships with any companies, whose products or services may be related to the subject matter of the article.

References

1. Mulita F, Anjum F. Thyroid Adenoma. Study Guide from StatPearls Publishing, Treasure Island (FL), 24 Sep 2020. Available from: https://europepmc.org/article/MED/32965923. Accessed 28 June, 2024.
2. Su W, Xu Y, Wang Y, et al. Comparison of disease burden factors of thyroid cancer between China and the world from 1990 to 2019. *Acta Academiae Medicinae Sinicae*. 2023;45(6):940–948. doi:10.3881/j.issn.1000-503X.15738
3. Haugen BR, Alexander EK, Bible KC, et al. 2015 American thyroid association management guidelines for adult patients with thyroid nodules and differentiated thyroid cancer: the American thyroid association guidelines task force on thyroid nodules and differentiated thyroid cancer. *Thyroid*. 2016;26(1):1–133. doi:10.1089/thy.2015.0020
4. Dudea SM, Botar Jid C. Ultrasound elastography in thyroid disease. *Med Ultrason*. 2015;17(1):74–96. doi:10.11152/mu.2013.2066.171.smd
5. Zhang Y-X, Xue J-P, Li H-Z, et al. Clinical value of shear wave elastography color scores in classifying thyroid nodules. *Int J Gen Med*. 2021;14:8007–8018. doi:10.2147/IJGM.S331406
6. Liu B-J, Zhang Y-F, Zhao C-K, et al. Conventional ultrasound characteristics, TI-RADS category and shear wave speed measurement between follicular adenoma and follicular thyroid carcinoma. *Clin Hemorheol Microcirc*. 2020;75(3):291–301. doi:10.3233/CH-190750
7. Kim HJ, Choi IH, Jin S, et al. Efficacy of shear-wave elastography for detecting postoperative cervical lymph node metastasis in papillary thyroid carcinoma. *Int J Endocrinol*. 2018;2018:1–6.
8. Borysewicz-Sanczyk H, Sawicka B, Karny A, et al. Suspected malignant thyroid nodules in children and adolescents according to ultrasound elastography and ultrasound-based risk stratification systems—experience from one center. *J Clin Med*. 2022;11(7):1768. doi:10.3390/jcm11071768
9. Wen X, Li B, Yu X, et al. Does shear wave elastography for medullary thyroid carcinoma predict lateral cervical lymph node metastasis? *Eur J Radiol*. 2022;146:110079. doi:10.1016/j.ejrad.2021.110079
10. Bryan RH. 2015 American thyroid association management guidelines for adult patients with thyroid nodules and differentiated thyroid cancer: what is new and what has changed? *Cancer-Am Cancer Soc*. 2017;123:372–381.
11. Liu Y, He L, Yin G, et al. Association analysis and the clinical significance of BRAF gene mutations and ultrasound features in papillary thyroid carcinoma. *Oncol Lett*. 2019;18(3):2995–3002. doi:10.3892/ol.2019.10641
12. Chen J, Li XL, Zhao CK, et al. Conventional ultrasound, immunohistochemical factors and BRAF(V600E) mutation in predicting central cervical lymph node metastasis of papillary thyroid carcinoma. *Ultrasound Med Biol*. 2018;44(11):2296–2306. doi:10.1016/j.ultrasmedbio.2018.06.020
13. Mulita F, Verras G, Dafnomili V, et al. Thyroidectomy for the management of differentiated thyroid carcinoma and their outcome on early postoperative complications: a 6-year single-centre retrospective study. *Chirurgia*. 2022;117(5):556–562. doi:10.21614/chirurgia.2736
14. Mulita F, Verras G, Anagnostopoulos C, et al. A smarter health through the internet of surgical things. *Sensors*. 2022;22(12):4577. doi:10.3390/s22124577
15. Zhao N, Yao M, Han R, et al. The diagnostic value of second ultrasound-guided fine-needle aspiration for thyroid nodules. *J Clin Ultrasound*. 2022;50(3):405–410. doi:10.1002/jcu.23119
16. Mulita F, Iliopoulos F, Tsilivigkos C, et al. Cancer rate of Bethesda category II thyroid nodules. *Med Glas*. 2022;19(1):1. doi: 10.17392/1413-21.

17. Dong Y, Mao M, Zhan W, et al. Size and ultrasound features affecting results of ultrasound-guided fine-needle aspiration of thyroid nodules. *J Ultrasound Med*. 2018;37(6):1367–1377. doi:10.1002/jum.14472
18. Chen J, Li XL, Zhang YF, et al. Ultrasound validation of predictive model for central cervical lymph node metastasis in papillary thyroid cancer on BRAF. *Future Oncol*. 2020;16(22):1607–1618. doi:10.2217/fon-2020-0069
19. Cao J, Huang W, Huang P, et al. ACR TI-RADS and ATA ultrasound classifications are helpful for the management of thyroid nodules located in the isthmus. *Clin Hemorheol Microcirc*. 2022;80(4):463–471. doi:10.3233/CH-211304
20. Zhang Y, Lu F, Zhang YF, et al. Predicting malignancy in thyroid nodules with benign cytology results: the role of Conventional Ultrasound, shear wave elastography and BRAF V600E. *Clin Hemorheol Microcirc*. 2021;81(1):33–45. doi:10.3233/CH-211337
21. Azizi G, Keller JM, Mayo ML, et al. Shear wave elastography and Afirma™ gene expression classifier in thyroid nodules with indeterminate cytology: a comparison study. *Endocrine*. 2018;59(3):573–584. doi:10.1007/s12020-017-1509-9
22. Li H, Kang C, Xue J, et al. Influence of lesion size on shear wave elastography in the diagnosis of benign and malignant thyroid nodules. *Sci Rep*. 2021;11(1):21616. doi:10.1038/s41598-021-01114-8
23. Zhang WB, Li JJ, Chen XY, et al. SWE combined with ACR TI-RADS categories for malignancy risk stratification of thyroid nodules with indeterminate FNA cytology. *Clin Hemorheol Microcirc*. 2020;76(3):381–390. doi:10.3233/CH-200893
24. Tan S, Sun PF, Xue H, et al. Evaluation of thyroid micro-carcinoma using shear wave elastography: initial experience with qualitative and quantitative analysis. *Eur J Radiol*. 2021;137:109571. doi:10.1016/j.ejrad.2021.109571
25. Liu X, Xie L, Ye X, et al. Evaluation of ultrasound elastography combined with chi-square automatic interactive detector in reducing unnecessary fine-needle aspiration on TIRADS 4 thyroid nodules. *Front Oncol*. 2022;12:823411. doi:10.3389/fonc.2022.823411
26. Zhou J, Zhan W, Chang C, et al. Breast lesions: evaluation with shear wave elastography, with special emphasis on the "stiff rim" sign. *Radiology*. 2014;272(1):63–72. doi:10.1148/radiol.14130818
27. Zhang L, Ding Z, Dong F, et al. Diagnostic performance of multiple sound touch elastography for differentiating benign and malignant thyroid nodules. *Front Pharmacol*. 2018;9:1359. doi:10.3389/fphar.2018.01359
28. Hu L, Liu X, Pei C, et al. Assessment of perinodular stiffness in differentiating malignant from benign thyroid nodules. *Endocr Connect*. 2021;10 (5):492–501. doi:10.1530/EC-21-0034
29. Mostoufi-Moab S, Labourier E, Sullivan L, et al. Molecular testing for oncogenic gene alterations in pediatric thyroid lesions. *Thyroid*. 2018;28 (1):60–67. doi:10.1089/thy.2017.0059
30. Dong X, Akuetteh PDP, Song J, et al. Major vault protein (MVP) associated with BRAFV600E mutation is an immune microenvironment-related biomarker promoting the progression of papillary thyroid cancer via MAPK/ERK and PI3K/AKT pathways. *Front Cell Dev Biol*. 2022;9:688370. doi:10.3389/fcell.2021.688370
31. Nucera C, Porrello A, Antonello ZA, et al. B-Raf V600E and thrombospondin-1 promote thyroid cancer progression. *Proc Natl Acad Sci USA*. 2010;107(23):10649–10654. doi:10.1073/pnas.1004934107
32. Kim TH, Park YJ, Lim JA, et al. The association of the BRAF V600E mutation with prognostic factors and poor clinical outcome in papillary thyroid cancer. *Cancer*. 2011;118(7):1764–1773. doi:10.1002/cncr.26500
33. Liang S, Huang K, Sun Y. Correlation between ultrasonographic appearance of papillary thyroid microcarcinoma and BRAF V600E mutation. *J Oncol*. 2022;2022:5916379. doi:10.1155/2022/5916379
34. Lee J-H, Lee E-S, Kim Y-S. Clinicopathologic significance of BRAF V600E mutation in papillary carcinomas of the thyroid. *Cancer*. 2007;110 (1):38–46. doi:10.1002/cncr.22754
35. Yip L, Nikiforova MN, Carty SE, et al. Optimizing surgical treatment of papillary thyroid carcinoma associated with BRAF mutation. *Surgery*. 2009;146(6):1215–1223. doi:10.1016/j.surg.2009.09.011
36. Krasner JR, Alyouha N, Pusztaszeri M, et al. Molecular mutations as a possible factor for determining extent of thyroid surgery. *J Otolaryngol Head Neck Surg*. 2019;48(1):51. doi:10.1186/s40463-019-0372-5
37. Nucera C, Nehs MA, Nagarkatti SS, et al. Targeting BRAFV600E with PLX4720 displays potent antimigratory and anti-invasive activity in preclinical models of human thyroid cancer. *The Oncologist*. 2011;16(3):296–309. doi:10.1634/theoncologist.2010-0317
38. Elisei R, Ugolini C, Viola D, et al. BRAFV600E Mutation and Outcome of Patients with Papillary Thyroid Carcinoma: a 15-Year Median Follow-Up Study. *J Clin Endocrinol Metab*. 2008;93(10):3943–3949. doi:10.1210/jc.2008-0607
39. Chen B, Shi Y, Xu Y, et al. The predictive value of coexisting BRAFV600E and TERT promoter mutations on poor outcomes and high tumour aggressiveness in papillary thyroid carcinoma: a systematic review and meta-analysis. *Clin Endocrinol*. 2021;94(5):731–742. doi:10.1111/cen.14316